A New Approach for the Synthesis of Nanostructured Polyurethane-Hydroxylapatite-based Hybrid Materials

Laura Mădălina Popescu[a,b], Roxana Mioara Piticescu[b], Tinca Buruiană[a], Eugeniu Vasile[c], Roxana Truşcă[c], and Viorel Bădiliţă[b]

[a] Romanian Academy, Institute of Macromolecular Chemistry "Petru Poni", 41A Grigore Ghica Voda Alley, Iasi, 6600, Romania
[b] National R& D Institute for Non-Ferrous and Rare Metals, 102 Biruintei Blvd., Pantelimon, 077145, Ilfov, Romania
[c] S.C. METAV C-D, Bucharest, Romania

Reprint requests to Dr. Laura Mădălina Popescu. Fax: +40213522048. E-mail: mpopescu@imnr.ro

Z. Naturforsch. **2011**, *66b,* 36 – 42; received September 2, 2010

The structural properties of composites prepared by a hydrothermal method in high-pressure conditions and the role of pressure in the formation of hydroxylapatite-polyurethane (HAp-PU) materials with strong interactions between the two components were investigated. X-Ray diffraction (XRD), high-resolution transmission electron microscopy (HRTEM), FT-IR and NMR analyses were used to characterize the composite powders from a structural, morphological and compositional point of view. Both FT-IR and NMR spectroscopies indicate interactions between hydroxylapatite and acid polyurethane.

Key words: Hybrid Composites, Nanoparticles, Hydrothermal Method, Infrared Spectroscopy, Transmission Electron Microscopy

Introduction

Inorganic-organic hybrid compounds offer the chance of designing materials which the present the advantages of both organic polymers and inorganic nanoparticles. Development of composite materials for bone tissue engineering has received considerable attention because the combination of bioactive ceramics such as calcium phosphates with polymers improves the mechanical properties of scaffolds. At the same time, the poor bioactivity of most polymers can be counteracted [1 – 4]. Both natural and synthetic polymers such as collagen, chitosan, poly(ethylene glycol), poly(L-lactide), poly(2-hydroxyethyl methacrylate), polyglycolic acid, poly-ε-caprolactone, polyethylene, polyether ether ketone (PEEK), and polyurethane have been used in combination with hydroxylapatite (HAp) to prepare organic-inorganic composite materials with interesting properties [1, 5 – 9]. However, a major challenge is to get a good chemical and/or physical binding between the polymer and the ceramic phase. Various methods for forming the composites have been devised. The most relevant fabrication techniques leading to 3-D composite scaffolds with highly interconnected pores are thermally induced phase separation (TIPS), solvent casting/particle leaching, solid-free form, microsphere sintering, and scaffold coating [1]. Kokubo's group developed a biomimetic process and found out that an HAp layer was formed on polymer films. Akashi's group prepared polymer-HAp composites by an alternating soaking process. These methods have also been used for the preparation of hydroxylapatite-polyurethane (HAp-PU) composites [10 – 17]. Wang *et al.* [18] reported a new HAp-PU composite porous scaffold developed by *in situ* polymerization. Therefore, coating and blending are the most common methods to modify polymers with an inorganic phosphate [4].

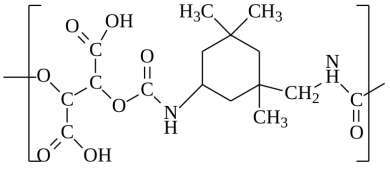

Fig. 1. Hard polyurethane-containing COOH groups.

The aim of the present work was to synthesize a new type of composite material based on carboxylic polyurethane and calcium phosphate using a hydrothermal method at high pressure, and to estab-

Table 1. Experimental parameters of the investigated samples.

Sample name	Sample type	HAp : PU molar ratio	Applied pressure (atm)
Sample 1	Acid PU	–	–
Sample 2	Hydroxylapatite	–	> 20
Sample 3	HAp-PU composite	4 : 1	> 20
Sample 4	HAp-PU composite	4 : 1	> 60
Sample 5	HAp-PU composite	1 : 4	> 60

lish the role of pressure in the formation of strong interactions between organic and inorganic components. Composition, structure and morphology of the resulting composite powders were investigated using XRD, SEM, and FT-IR techniques.

Experimental Section

A hard polyurethane with 537 meq COOH groups/100 g polymer and M_w (GPC) = 9200 Da was synthesized as it was described in ref. [19], its chemical structure being presented in Fig. 1. This polymer was dissolved in *N*,*N*-dimethylacetamide 99.5 % p. a. (c = 5 %).

Preparation of HAp-PU composite material

Purity grade hydroxylapatite precursors, namely calcium nitrate tetrahydrate and ammonium dihydrogen phosphate were solubilized in water under a strict pH control, adding ammonium hydroxide as a mineralizing agent. The aqueous suspension thus obtained was further mixed with the polymer solution under vigorous stirring, followed by a hydrothermal reaction in a Cortest autoclave, USA. Reactions were conducted in a closed system at low temperature ($T <$ 100 °C) and high pressure ($P >$ 20 atm) leading to nanostructured composite powders. The detailed hydrothermal synthesis process is described in our previous work [19]. Experimental parameters of the investigated samples are presented in Table 1.

Characterizations

The structural characterization was performed on a Bruker D8 Advance diffractometer using CuK_α radiation, the Diffrac^{plus} XRD Commender (Bruker AXS) software and the Bragg-Brentano diffraction method. Morphological observation of the hydrothermally prepared composite was carried out by electron microscopy using a Tecnai G2 F30 S-Twin Field Emission High Resolution Transmission Electron Microscope (HRTEM), with a 50 – 300 kV electron source and magnifications of 58 x-970 kx (TEM) and 150 x-230 Mx (STEM). The calcium and phosphorus contents in HAp-PU composites was determined by an atomic absorption spectrometer AAS ZEEnit 700, Analytic Jena AG, Germany, and an inductively coupled plasma ICP spectrometer Spectroflame P, Germany, respectively. The chemical structures of the composite materials were confirmed by analyzing the FTIR spectra. FTIR spectra were recorded in the transmission mode on an ABB MB 3000 spectrometer from 4000 to 550 cm^{-1}, averaging 64 scans at a resolution of 4 cm^{-1}. The solid samples were carefully mixed with KBr powder for 30 min. A homogeneous mixture of about 1 % sample in KBr powder was obtained. Quantitative Fourier-transformed infrared spectra were collected using the PIKE Technologies EasiDiff diffuse reflectance accessory. The HORIZON^{MB} software was used for automatic data processing.

Table 2. Mean crystallite size determined by XRD.

Sample code	Sample 2	Sample 3	Sample 4	Sample 5
[00l] Crystallite size (Scherrer), nm	58	27	34.3	16.6
[hkl] Isotropic crystallite size (Scherrer), nm	25	11	11.1	5.8

Results and Discussion

Experiments performed in this study were focused on the investigation of the structural properties of the composites prepared by the hydrothermal method in high-pressure conditions following mainly the role of pressure in the formation of HAp-PU materials through strong interactions between the two components. High-pressure synthesis could lead to structural and conformational changes of the materials, including a possible increase of H bond density in the polymer structure. The chemical structure was studied by FTIR spectroscopy, and the results were corroborated with those obtained by physical characterization, *i. e.* XRD and HRTEM techniques.

XRD analysis

XRD patterns of the investigated samples are presented in Fig. 2. XRD studies revealed that the properties of the HAp crystallites of composite samples are strongly dependent on the parameters of the synthesis.

The mean crystallite size obtained from XRD patterns by the Scherrer formula are presented in Table 2.

The crystallite size decreased upon adding the polymer component when the same pressure was used in the synthesis (samples 2 and 3), whereas for the same composition (samples 3 and 4) an increase of the pressure led to crystallites with larger size. Smaller HAp nanocrystals were obtained in samples with a high polymer content and under higher pressure (sample 5). HAp crystallites of sample 4 have a preferential growth

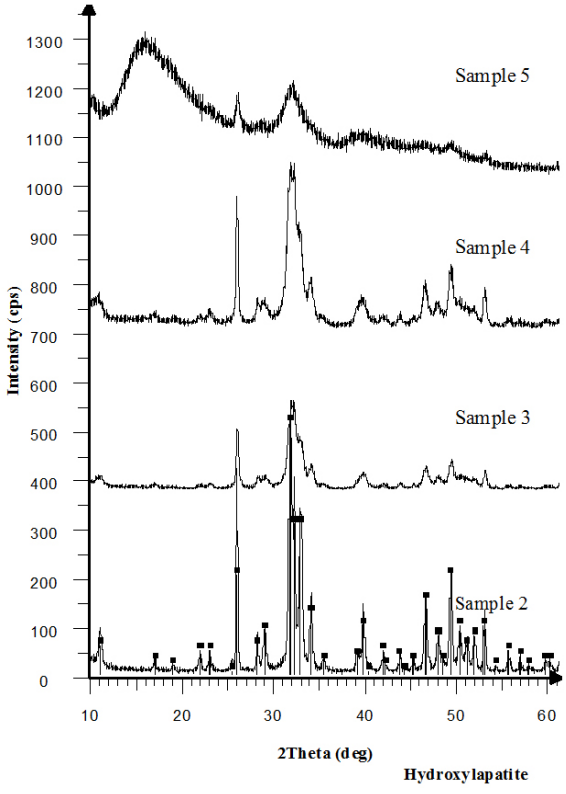

Fig. 2. X-Ray diffraction patterns of samples 2, 3, 4 and 5.

in the (00l) direction, leading to columnar crystals with a height/width ratio of 3/1. It can be observed that the cell parameter a of sample 4 is a little larger than the theoretical cell parameter of hydroxylapatite, $Ca_5(PO_4)_3(OH)$, a_{obs} = 9.450 Å and a_{PDF} = 9.418 Å, indicating some disorder in the arrangement of atoms in the basal plane of the hexagonal structure.

The increase of the cell parameter a is more pronounced in the case of sample 5 where a_{obs} = 9.543 Å and a_{PDF} = 9.418 Å. This may be correlated with the mean crystallite size.

HRTEM characterization

HRTEM images (Figs. 3 and 4) show the morphological patterns of the composites and their structural characteristics influenced by the composition.

A low magnification micrograph of sample 4 (Fig. 3a) displays the typical nanostructure of hydroxylapatite crystallized as nano-whiskers. Polyurethane covers the hydroxylapatite nanoparticles and can be only visualized at high magnifications (Fig. 4b) as an amorphous phase. FFT processing of the image (Fig. 3b) emphasizes the existence of fringe contrast corresponding to the families of crystalline planes of the compound $Ca_5(PO_4)_3(OH)$ with hexagonal crystal lattice.

Table 3. Chemical composition of HAp-PU composites.

	Chemical composition (% weight)				
	Sample 4		Sample 5		Hydroxyl-apatite
Element	Spectrometry	EDX	Spectrometry	EDX	Theoretic
Ca	29	37.2	12.6	12.8	39.8
P	15.6	18.4	5.6	5.5	18.5
C	10	9	58.6	69.7	–
N	–	1.1	–	2.4	–
O	–	34.3	–	9.6	–
Ca : P ratio	1.44	1.57	1.74	1.82	1.67

In the case of composites with a polymer matrix and HAp (molar ratio 1 : 4), the structure is different. Very fine hydroxylapatite nano-whiskers are incorporated into large polyurethane particles (Fig. 4b), and these are not completely crystallized. A porous structure with superposed layers of the polymer and HAp embedded in polyurethane is formed (Fig. 4a). A crystalline plane of hydroxylapatite was not observed in this case because of the amorphous polymer layers.

X-Ray energy dispersive spectra of HAp-PU composites (Fig. 5) revealed the presence of calcium, phosphorus, carbon, nitrogen and oxygen in all the samples. Ca : P atomic ratios of samples 4 and 5 were calculated both from AAS or ICP spectroscopies (high accuracy methods) and EDX analysis (lower accuracy method), and the results are presented in Table 3.

As one can see, the Ca : P atomic ratio for sample 4 (HAp : PU = 4 : 1 molar ratio) was slightly lower than the theoretical value of 1.67 for stoichiometric hydroxylapatite $Ca_{10}(PO_4)_6(OH)_2$. For sample 5 (HAp : PU = 1 : 4 molar ratio) a higher Ca : P atomic ratio suggested an amorphous calcium phosphate.

The high-resolution transmission electron micrographs depicted in Fig. 6 confirm the hypothesis that the microstructure of the composites is influenced by their composition. In Fig. 6a crystalline planes of hydroxylapatite can be observed as well as a disordered structure due to the polyurethane particles. In Fig. 6b the amorphous phase predominates, and the growth of HAp whiskers is initiated.

FTIR analysis

FTIR spectroscopy has been used to study the interactions of COOH functional groups of polyurethane

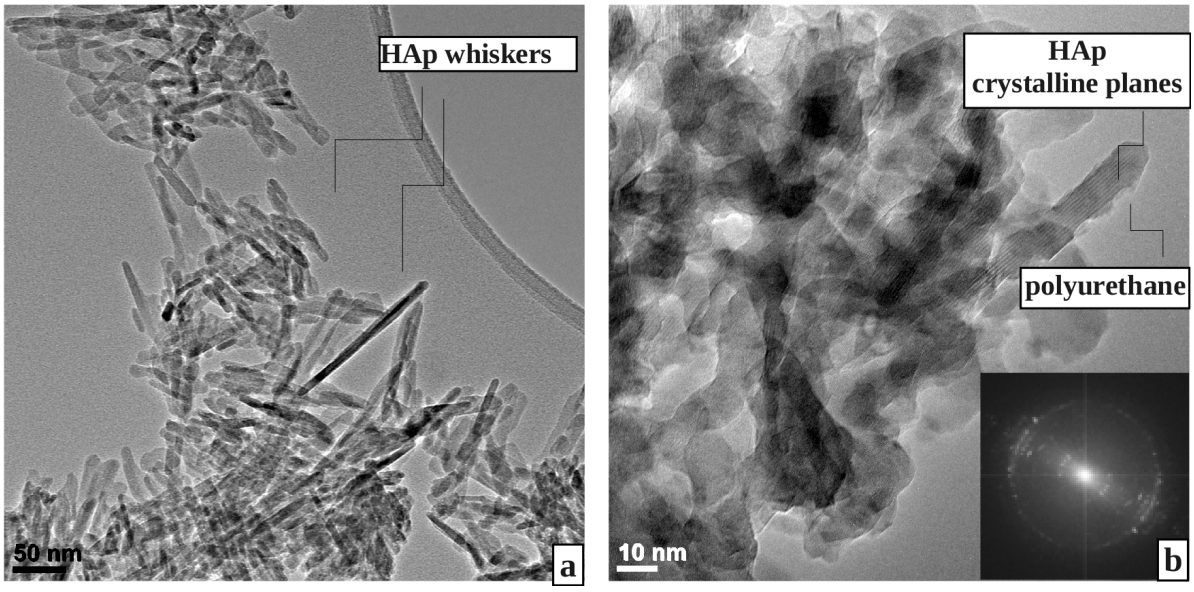

Fig. 3. HRTEM images of sample 4 (HAp-PU composite with HAp matrix) at different magnifications: a) 50 nm. Columnar hydroxylapatite crystals are observed; b) 10 nm. The corresponding Fast Fourier Transform (FFT) image is presented in the right corner.

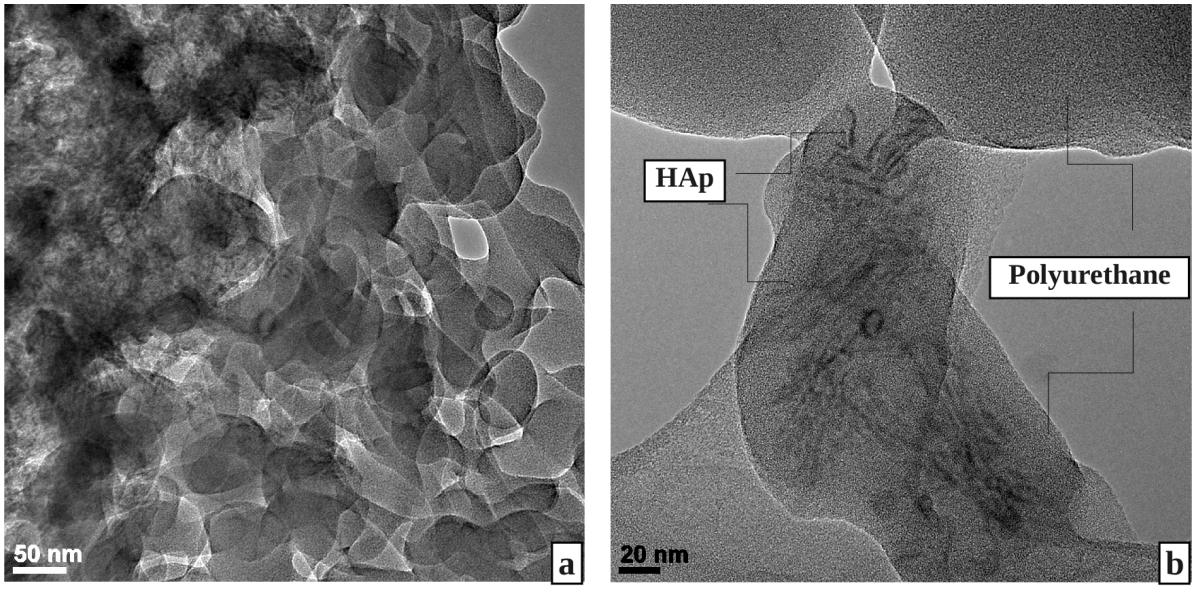

Fig. 4. HRTEM images of sample 5 (HAp-PU composite with polymer matrix) at: (a) 50 nm. Hydroxylapatite entrapped in a polymer matrix is observed above the main diagonal; (b) 20 nm. Rare HAp whiskers are observed below the main diagonal. Large polyurethane particles are prevalent.

with hydroxylapatite and to demonstrate the formation of a homogeneous composite. The FTIR spectra of some representative samples are depicted in Fig. 7.

As one can see from Fig. 7, the characteristic peaks of hydroxylapatite are present in the $1110-900\ \mathrm{cm}^{-1}$ range (fingerprint region) of hydrothermally synthesized composites, irrespective of the polymer content.

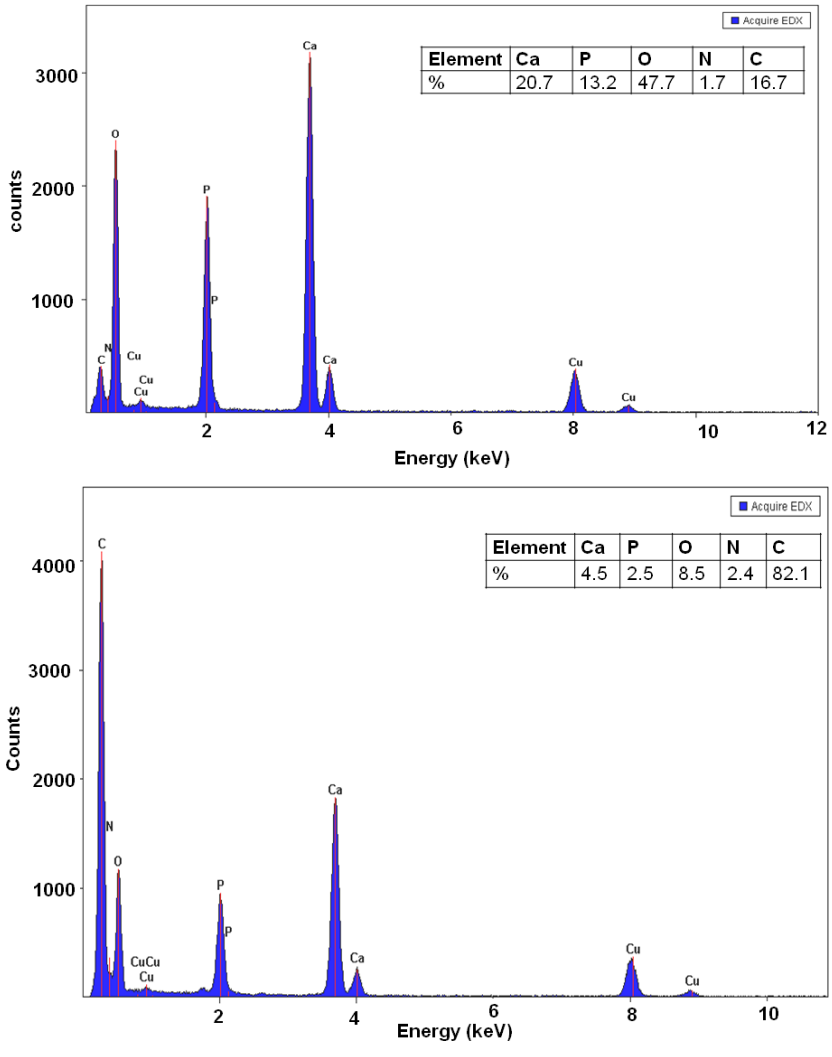

Fig. 5. EDAX spectra of some representative composites and atomic composition; above: associated with the image of Fig. 3a; below: associated with the image of Fig. 4b.

Yet, the $\nu(PO_4{}^{3-})$ vibration at 962 cm^{-1} is weak for composites with an organic matrix (sample 5). The ν(OH) stretching vibration is blocked in composites with a polymer matrix (sample 5). The intensity of the OH band decreases with increasing pressure.

On the other hand, amide I and amide II bands at 1634 and 1558 cm^{-1}, respectively, were identified in sample 5. Samples 3 and 4 present broader peaks in the region of the amide I band probably due to some interactions with the $PO_4{}^{3-}$ group. The band corresponding to the amide II vibration is slightly shifted to 1550 cm^{-1} and has a low intensity. The band at 1746 cm^{-1}, which was assigned to C=O groups, has almost disappeared in HAp-PU composites, and only a small shoulder could be observed at 1722 and 1718 cm^{-1} in samples 4 and 5, respectively. One can suppose that the C=O groups interact with Ca^{2+} ions of hydroxylapatite. CH_2 and CH_3 stretching vibrations in the 2954 – 2842 cm^{-1} region are also present in the spectra of all the samples, their intensity increasing with pressure.

In order to demonstrate the polymer's presence in HAp-PU composites, the peak area ratio for two characteristic bands of polyurethane was calculated taking as standard the amide I band at 1634 cm^{-1} in sample 1. The peak areas corresponding to the ν(C=O) and δ(NH) bands of samples 1, 3, 4, and 5 were divided by the peak area corresponding to the amide I band, as presented in Table 4.

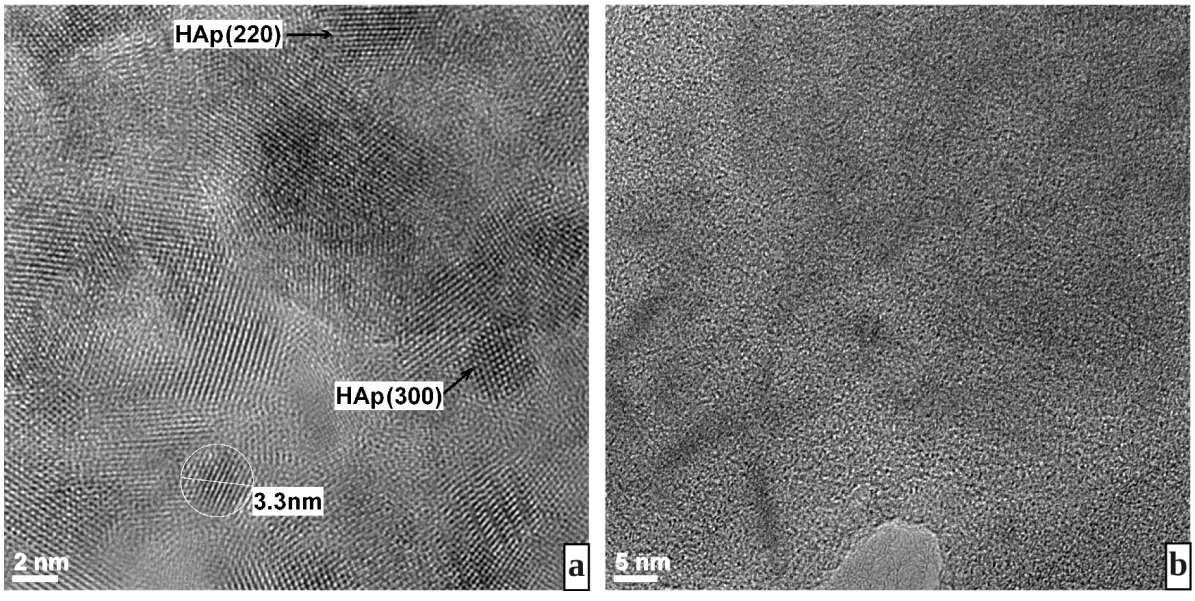

Fig. 6. HRTEM image of: a) sample 4, length scale 2 nm; b) sample 5, length scale 5 nm.

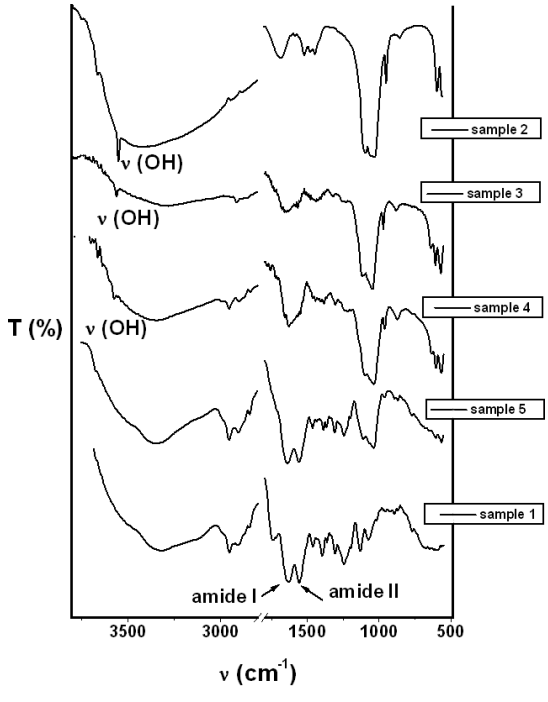

Fig. 7. FT-IR spectra of HAp-PU composites in the range of 4000 – 2800 cm^{-1} and 1800 – 500 cm^{-1}.

The peak area ratio of C=O bands decreases significantly in the case of HAp-PU composites, compared to a polyurethane sample. This could be a consequence of carbonyl groups interacting with hydroxylapatite. In the case of the amide II band, the peak area ratios of composite samples also decrease compared to sample 1 (PU). As the polymer content is lower, the peak area ratio is also lower.

Table 4. The peak area ratio of HAp-PU composites using the amide I band of the initial polymer at 1634 cm^{-1} as standard.

Sample	Peak area ratio	
1	$A_{1746}/A_{1634} = 0.35$	$A_{1558}/A_{1634} = 0.87$
5	$A_{1718}/A_{1638} = 0.05$	$A_{1558}/A_{1638} = 0.51$
4	$A_{1762}/A_{1630} = 0.02$	$A_{1550}/A_{1630} = 0.28$
3	–	$A_{1550}/A_{1634} = 0.24$

Table 5. The peak area ratio of HAp-PU composites using the $\nu(PO_4{}^{3-})$ band of HAp at 1038 cm^{-1} as standard.

Sample	Peak area ratio	
2	$A_{1094}/A_{1038} = 0.79$	$A_{962}/A_{1038} = 0.13$
4	$A_{1094}/A_{1038} = 0.77$	$A_{962}/A_{1038} = 0.09$
3	$A_{1106}/A_{1038} = 0.56$	$A_{962}/A_{1038} = 0.06$
5	$A_{1110}/A_{1038} = 0.55$	$A_{962}/A_{1038} = 0.02$

Similarly, to demonstrate the hydroxylapatite presence in composite samples, the peak area ratio of two characteristic HAp bands was calculated taking as standard the $\nu(PO_4{}^{3-})$ band at 1038 cm^{-1}. Results are presented in Table 5.

In this case, the peak area ratios related to phosphate bands show that PO_4 groups are present in the composite samples, so one can suppose that Ca ions

are involved in organic-inorganic interactions with acid polyurethane.

Conclusion

Nanostructured composites based on hydroxylapatite and ionic polyurethane (molar ratios of 4 : 1 and 1 : 4) were prepared under hydrothermal conditions at low temperatures and high pressures. The former organic/inorganic composites showed HAp crystallites with a size of around 30 – 60 nm surrounded by polyurethane particles, while in the latter there are fine hydroxylapatite nano-whiskers incorporated into large polyurethane particles. FTIR data suggest the existence of interactions between the hydroxylapatite and the acid polyurethane leading to the formation of composite structures.

Acknowledgement

The authors (L. M. P. and T. B.) would like to thank for the financial support of the European Social Fund – "Cristofor I. Simionescu" Postdoctoral Fellowship Programme (ID POSDRU/89/1.5/S/55216), Sectorial Operational Programme Human Resources Development 2007 – 2013.

[1] K. Rezwan, Q. Z. Chen, J. J. Blaker, A. R. Boccaccini, *Biomaterials* **2006**, *27*, 3413 – 3431.
[2] Y. Zhu, D. X. Sun, H. Zheng, M. Wei, L. M. Zhang, *J. Mater. Sci.* **2007**, *42*, 545 – 550.
[3] D. W. Hutmacher, J. T. Schantz, C. X. F. Lam, K. C. Tan, T. C. Lim, *J. Tissue Eng. Regen. Med.* **2007**, *1*, 245 – 260.
[4] M. N. Huang, Y. L. Wang, Y. F. Luo, *J. Biomed. Sci. Eng.* **2009**, *2*, 36 – 40.
[5] T. Takayama, M. Todo, A. Takano, *J. Mechan. Behavior Biomed. Mater.* **2009**, *2*, 105 – 112.
[6] J. M. Oliveira, M. T. Rodrigues, S. S. Silva, P. B. Malafaya, M. E. Gomes, C. A. Viegas, I. R. Dias, J. T. Azevedo, J. F. Mano, R. L. Reis, *Biomaterials* **2006**, *27*, 6123 – 6137.
[7] A. S. Khan, Z. Ahmed, M. J. Edirisinghe, F. S. L. Wong, I. U. Rehman, *Acta Biomaterials* **2008**, *4*, 1275 – 1287.
[8] C. X. Zhao, W. D. Zhang, *Eur. Polymer J.* **2008**, *44*, 1988 – 1995.
[9] M. Wang, W. Bonfield, *Biomaterials* **2001**, *22*, 1311 – 1320.
[10] M. W. Laschke, A. Strohe, M. D. Menger, M. Alini, D. Eglin, *Acta Biomater.* **2010**, *6*, 2020 – 2027.
[11] Z. Dong, Y. Li, Q. Zou, *Appl. Surf. Sci.* **2009**, *255*, 6087 – 9160.
[12] A. Asefnejad, A. Behnamghader, M. T. Khorasani, *Biomed. Eng.* **2010**, *1* and *2*, 680.
[13] L. Fang, P. Gao, Y. Leng, *Composites: Part B* **2007**, *38*, 345 – 351.
[14] C. I. R. Boissard, P. E. Bourban, A. E. Tami, M. Alini, D. Eglin, *Acta Biomater.* **2009**, *5*, 3316 – 3327.
[15] M. Wang, *Biomaterials* **2003**, *24*, 2133 – 2151.
[16] N. M. K. Lambda, K. A. Woodhouse, S. L. Cooper, *Polyurethanes in Biomedical Applications*, CRC Press, New York, **1998**, pp. 43 – 86.
[17] K. D. Kavlock, T. W. Pechar, J. O. Hollinger, S. A. Guelcher, A. S. Goldstein, *Acta Biomater.* **2007**, *3*, 475 – 484.
[18] L. Wang, Y. Li, Y. Zuo, L. Zhang, Q. Zou, L. Cheng, H. Jiang, *Biomed. Mater.* **2009**, *4*, 025003.
[19] R. M. Piticescu, T. Buruiana, N. Plesu, E. Vasile, C. Moldovan, B. Fartat, C. Rusti, *Optoelectr. Adv. Mater. Rapid Commun.* **2010**, *4*, 401 – 406.